Wear 460–461 (2020) 203353

Contents lists available at ScienceDirect

Wear

journal homepage: http://www.elsevier.com/locate/wear

Avoiding the initial adhesive friction peak in fretting

Janne Juoksukangas [a,*], Jouko Hintikka [b,a], Arto Lehtovaara [a], Antti Mäntylä [b], Joona Vaara [b], Tero Frondelius [b,c]

[a] Tribology and Machine Elements, Materials Science and Environmental Engineering, Faculty of Engineering and Natural Sciences, Tampere University, P.O. Box 589, FI-33014 Tampere University, Finland
[b] R&D and Engineering, Wärtsilä, P.O. Box 244, 65101 Vaasa, Finland
[c] University of Oulu, Erkki Koiso-Kanttilan katu 1, 90014 Oulu, Finland

ARTICLE INFO

Keywords:
Fretting
Friction
Lubrication
Third body layer
Fretting wear

ABSTRACT

An initial friction peak typically occurs in a dry self-mated quenched and tempered steel fretting contact in gross sliding conditions. The peak is related to adhesive friction and wear, which causes non-Coulomb friction. An early surface degradation including cracks may occur. To avoid such a peak, different media were studied using a flat-on-flat fretting test device with a large annular contact. All the media decreased the initial friction peak in comparison to the dry reference case, and in one series the peak was completely removed. The peak could often be delayed by lubrication. The steady-state coefficient of friction values mostly remained at similar levels to those of the dry contact, but decreased when oil was applied. Nevertheless, some surface damage occurred in every test, with varying amounts of wear.

1. Introduction

Fretting is characterised as small amplitude cyclic rubbing between surfaces in contact that can cause fretting fatigue and fretting wear. Fretting fatigue can notably decrease fatigue life and lead to early failure in machines and other applications. The rubbing can be caused by loads being transmitted along the contact interfaces in assemblies, or by vibrations. The sliding amplitudes typically range from a few micrometres up to some tens or hundreds of micrometres. In a gross sliding condition, the whole nominal contact area is sliding. Sometimes however, only a part of the nominal contact area is sliding, and this is called a partial-slip sliding condition. There is also, in fact, a mixed fretting regime which encompasses both of these conditions during its loading history. The coefficient of friction (hereafter '*COF*') is known to be high in fretted contacts, whatever pair of materials is in contact. Thus, shear tractions increase and consequently, stresses in the contact. Ultimately, this can lead to cracking and wear. It is generally acknowledged that non-idealities in fretting [1] make fretting a challenging phenomenon.

Many palliatives, such as lubrication, have been proposed to alleviate fretting damage. In the field of tribology, lubrication is an efficient way to decrease friction between sliding contacts and to decrease wear. For example, greases are often used to improve fretting behaviour in steel ropes or even electrical connectors [2]. Numerous fretting studies have shown that greases [3] and oils [4,5] not only decrease *COF* but also decrease the amount of wear compared to a dry contact [3,6,7]. Lubrication has been proved to either delay or eliminate the initial peak of *COF* before stabilization [5]. However, it has also been shown that lubrication can only decrease *COF* significantly during the initial loading cycles [8]. Circulating lubricant is also beneficial because it may also transfer wear debris away from the contact [9]. It seems certain that the amount of available oxygen in the contact can have a significant effect on fretting wear. The adhesion increases notably in nitrogen due to the lack of an oxide layer, although the wear rate can be lower than in air [9]. An important role for the lubricant is to limit the amount of oxygen in the contact [5,9], as this limits oxidization of the debris from the fretting wear. It appears that grease is a better oxygen inhibitor than oil [10]. If oxidation can be prevented or even reduced, this can result in steels with larger dark grey regions in the fretted surfaces, rather than an overall orange-red coloration [5].

However, lubrication does not necessarily have only positive effects on fretting. In practice, a lubricated contact can increase slip by increasing frictional energy dissipation and thus, the amount of wear. It has been shown that accumulated dissipated energy correlates with wear volume in lubricated fretting contact conditions [11]. Nevertheless, lubrication may decrease tangential forces, and in turn, decrease dissipated energy and wear, as well as friction-induced stresses. It can

* Corresponding author.,
E-mail address: janne.juoksukangas@tuni.fi (J. Juoksukangas).

https://doi.org/10.1016/j.wear.2020.203353
Received 26 November 2019; Received in revised form 9 April 2020; Accepted 19 May 2020
Available online 22 May 2020

also change the wear mechanism [7]. Zhou et al. [8] have suggested that oil may penetrate into surface cracks leading to a higher risk of debris becoming detached, which also increases wear.

The viscosity of the lubricant and the operating parameters both have an effect on the lubrication state in fretting conditions [11]. *COF* has been observed to increase as the viscosity of the lubricant increases, though the relationship is not quite linear [12]. Similar behaviour was also observed in Ref. [10] after the initial loading cycles. In addition, increased fretting loading frequency can diminish lubrication and increase *COF* [2]. Within sliding amplitudes of a few micrometres, a dry contact had the lowest *COF,* but when the slip was increased, the lubricated contact had the lowest *COF* [12]. The lubricant may be removed from the contact by the fretting motion, leading to decreased lubrication conditions, but on the other hand, penetration of a new lubricant is possible [2]. Qin et al. [13] observed that oil penetration into the contact was less effective in more-conforming contacts. A lubricant may be removed from the central contact zone during cyclic loading, but it may still 'isolate' the contact [5]. However, even if the fretting contact is lubricated, metal-to-metal contact is almost sure to happen [5].

Solid lubricants can be effective in terms of *COF* and wear in fretting. Graphite in oil can decrease wear compared to an oil lubricated condition [5]. MoS_2 and graphite coatings effectively decreased the *COF* during the initial loading cycles, though the *COF* started to increase when the coating was worn [14]. Solid lubricants have been considered more suitable in small sliding conditions (partial slip condition) whereas grease and oil lubrication are more suitable at higher sliding magnitudes (gross sliding) [2].

Fretting in steels is characterized by a reddish-brown 'cocoa' wear debris. Even if the contact surfaces are initially in contact and the relative motion is initiated by a mechanism such as shear, fretting induces oxidized wear debris that forms a third body layer between the surfaces [15], allowing the motion to be adapted via a velocity accommodation mechanism [16]. This prevents direct metal-metal contact and decreases adhesion. As a result, the main wear mechanism may change from adhesion to abrasion. Basically, if the adhesive wear is dominant, the worn particles are useful, but in the case of abrasive wear they contribute to the degree of wear [17].

Corrosive conditions change frictional behaviour and the presence of corrosion products may change the dominating wear mechanism [18]. Fretting experiments in a flat-on-flat contact revealed that wear was lower in artificial seawater containing mainly NaCl than it was in filtered water, indicating that the corrosion products acted as a lubricant [18]. An oil-lubricated contact still had the lowest wear. Dry contact conditions led to the highest wear, and even pure water decreased wear. The results for the *COF*s were similar, as the steady state *COF* was highest in the dry contact and decreased in both types of water. However, the lowest *COF* was clearly observed in the oil-lubricated contact. In another study, the *COF* also decreased when water containing chlorides, such as sodium chloride, was used compared to pure water [19]. However, wear had the opposite behaviour. Compared to the dry and grease-lubricated wire rope contacts, the lowest *COF* was achieved in experiments with the NaCl solution [20].

Initially-peaking *COF* has not only been observed in dry gross-sliding fretting experiments using self-mated quenched and tempered ('QT') steel specimens [21], but also with cast iron and structural steel [22,23]. The experiments with QT have shown that *COF* increases over unity, as high as 1.5, within the first few hundreds or thousands of loading cycles. After peaking, *COF* stabilises to values at about 0.7–0.8. The initial peak in *COF* has been related to adhesive friction and wear causing non-Coulomb friction [24]. In non-Coulomb conditions, friction force in gross sliding increases as the turning point is approached. In ideal conditions, the friction force remains constant. Adhesive wear causes protrusions and depressions on the surface which are tangentially interlocked [24]. Adhesive material transfer 'spots' [21,25] contain severe damage in terms of wear, plastic deformation, tribologically transformed structure and cracks, already observable within the initial loading cycles [26,27].

As the initial high friction peak is linked to non-Coulomb friction and fretting damage, further approaches to avoiding such a peak have been assessed. It has already been demonstrated that a preceding running-in phase with small sliding amplitude before the gross sliding phase can diminish the friction peak [28,29]. In addition, the concept of stable friction [30] determines the level above which the friction starts to peak. In this study, different media and intermediate layers between the fretting contact surfaces were studied using self-mated quenched and tempered steel specimens. The ultimate goal of these media would be to separate the contacting surfaces, thus preventing direct metal-to-metal contact. The main focus was to study the fretting-induced frictional behaviour, and the fretting damage in terms of fretting scar inspections and wear characterization. An annular type of contact was used that has large nominal contact area and no geometrical edges in the sliding directions. Thus, this may reasonably emulate practical contacts, such as bolted joints and interference fits. Three different oils and greases were studied: an engine oil and a gear oil and a grease with graphite and EP additives. Copper and molybdenum sulphide pastes were also used. In addition, an artificial debris layer (third body layer) was imposed on the test surfaces, and pre-corroded specimens were also studied. This is a full-length article from an extended abstract [31] with additional experiments.

2. The experiments

2.1. The test device

An annular-type fretting test device was used in the study, which has been comprehensively presented elsewhere [21], and only a brief overview is given here. This consists of two similar flat-ended specimens forming a nominal contact area of 314 mm^2. The inner r_i and outer r_o radiuses of the specimens are 7.5 mm and 12.5 mm, respectively. The specimens and the whole device with scale bars are shown in Fig. 1.

The specimens are under static normal load created by a hydraulic cylinder. One specimen is fixed to the frame of the device and the second is cyclically rotated around the central axis, which in turn creates slip between the specimens (Fig. 1). The cyclic (oscillating) rotation at a frequency of 40 Hz is created with an electric vibrator via a lever arm. The test device allows the use of a wide variety of nominal normal pressures and sliding amplitude values.

The cyclic rotation of the specimen is measured and elastic deformations are extracted from the measurements to determine the actual sliding amplitude, u_a, at the contact. This measurement is also used to control the rotation actuator, meaning that the device is displacement controlled. The normal load *P* and frictional torque *T* are also measured. Other measured signals are presented in Ref. [21]. The maximum *COF* ('COF_{max}') is determined from the measured maximum torque (*T*) value during a loading cycle and normal pressure distribution *p(r)*, as shown in Equation (1),

$$COF_{\max} = T \Big/ \left[2\pi \int_{r_i}^{r_o} r^2 \times p(r) dr \right] \quad (1)$$

The normal pressure distribution in radial direction has been calculated using the finite element method and it holds about 18% higher value at the inner radius r_i and about 18% lower value at the outer radius r_o, compared to the average normal pressure value. However, constant normal pressure can be assumed, as the resulting error is smaller than 1% [30]. The mean *COF* ('COF_{mean}') is based on the frictional energy dissipation *Ed*, which is the work done by the frictional contact and coincides with the area inside a fretting loop over one loading cycle. The loop is formed by the frictional torque and angle of rotation θ, which are both measured. $COF_{m_{ean}}$ is calculated from the

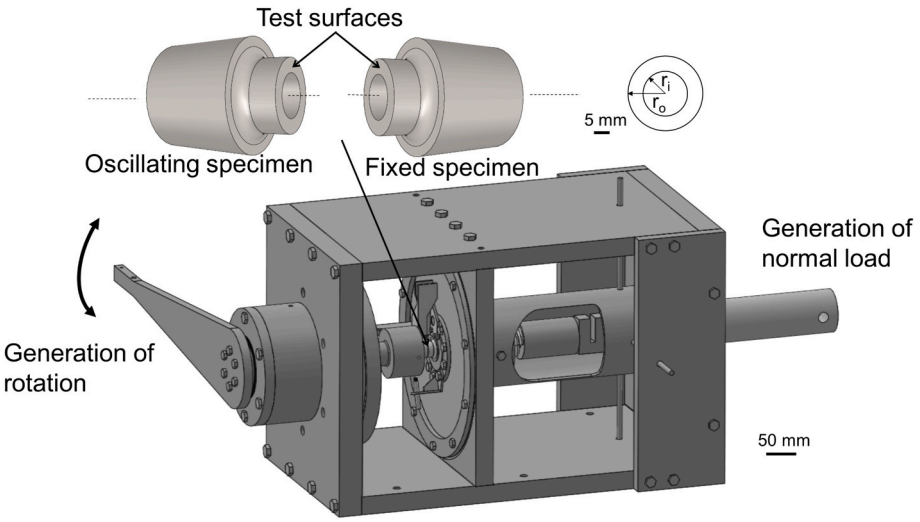

Fig. 1. The annular flat-on-flat fretting test device and the test specimens used.

accumulated dissipated energy *Ed*, rotation amplitude θ_a, and *p(r)*, as shown in Eq. (2).

$$COF_{mean} = Ed \Big/ \left[8\pi \int_{r_i}^{r_o} r^2 \times \theta_a \times p(r) dr \right] \quad (2)$$

The difference between the maximum and mean *COF*s, ΔCOF (i.e., $\Delta COF = COF_{max}$ - COF_{mean}), is used to indicate the level of non-Coulomb friction [24]. The higher the ΔCOF, the higher the level of non-Coulombness.

2.2. Materials and test specimens

The specimens were manufactured from quenched and tempered steel, EN-10083-1-34CrNiMo6+QT. The contact surfaces were ground leading to circular scratching marks in parallel with the fretting motion. The arithmetical mean surface roughnesses, *Sa*, of the contact surfaces were between 0.18–0.29 μm. The properties and numbers of tests of all the studied media are listed in Table 1. Viscosity and NLGI class are provided by the manufacturers.

Both the motor oil (Oil A) and the gear oil (Oil B) are synthetic and the gear oil has EP additives. The viscosities of the aforementioned oils are 5.6 mm^2/s and 15 mm^2/s (both at 100°), respectively. The base mineral oil viscosity of the grease (Grease) is 280 mm^2/s at 40 °C and it has a lithium thickener and the NLGI classification of the Grease is two.

Table 1
The media studied, their series names used in the study and the number of tests.

Name	Series name	Number of tests
Engine oil	Oil A	2
Gear oil (extreme pressure)	Oil B	1
Copper paste	Paste A	2
Lubricant paste incl. molybdenum sulphide	Paste B	2
Grease with EP additives and graphite	Grease	2
Pre-added fretting debris	PreTBL	2
Pre-corroded specimens	PreCorr	3

The copper paste (Paste A) has semi-synthetic base grease and it is intended to withstand high temperatures and pressures in practical use. The assembly paste (Paste B) contains molybdenum sulphide and it is intended to resist seizing up when the machine parts are being assembled.

2.2.1. Test procedure

The specimens were washed in an ultrasonic cleaner before applying any action using first acetone followed by ethanol. The same cleaning procedure was applied after testing before any post-analysis. The cleaned specimens were weighed before and after testing with a precision scales, Precisa EP 420A to quantify the amount of wear. Fig. 2 shows schematically the arrangement when applying oils (A) and the

pastes and the grease (B).

Special specimen clamping screws were used to allow the oil to flow freely to the contact through the screw (Fig. 2). An oil reservoir was placed above the test device and the screws were sealed to avoid external leakage. This arrangement creates insignificant hydrostatic pressure compared to contact loads. When starting the tests, the normal load was applied and the contact closed once the internal space in the specimens was filled with oil. In this way, the oil was spread completely all over the contact interface. Naturally, the inside edges of the specimens were in oil, but the outer edges were surrounded by the atmosphere, though the outer surfaces had some traces of oil on them. In the case of the grease and pastes, those were initially applied into the gap between the specimen contact surfaces before applying the normal load. When the normal load was applied, any excess medium was squeezed out of the contact, and this remained around the contact interface as shown schematically by the patches in Fig. 2B.

Wear debris collected from previous dry fretting tests with the same test device and using the same steel was mixed with ethanol and applied to the specimen's contact surface to create an artificial debris layer (labelled as 'PreTBL'). After the solvent had dried, the contact was closed by the normal load and a test started. Pre-corroded specimens ('PreCorr') were submerged in sodium hypochlorite (NaClO) for several hours before testing. The specimens were left to dry before testing. Corrosion products were present all over the contact surface. The counter specimen was un-corroded. Otherwise, the same test routine [21] was followed in all of these tests. A total of fourteen experiments were carried out in gross sliding conditions with a sliding amplitude of 35 μm and nominal normal pressure of 30 MPa. The evenness of the normal pressure distribution for every test was checked and adjusted using a pressure-sensitive film. Each test lasted for three million loading cycles. The rotation amplitude (sliding amplitude) was ramped up during the first 400 loading cycles. The tests were carried out in typical laboratory-room conditions. The results are compared with the reference tests in dry contact conditions which had the same sliding amplitude and normal pressure. These tests were carried out and published earlier [21]. After testing, the contact surfaces (fretting scar) were analysed using a field emission scanning electron microscope FESEM (Zeiss ULTRAplus) with an energy dispersive spectrometer EDS (Oxford Instruments XMaxN).

3. Results

3.1. Frictional behaviour

Fig. 3 shows the COF_{max} values of all the test carried out. The results for the oils are on the left, the pastes and grease in the middle and the artificial debris layer and pre-corroded specimens on the right. The vertical dotted line is at the point of 400 loading cycles showing the rotation ramping-up phase. The curves are presented after 100 loading cycles where the contact is already in gross sliding conditions (except PreTBL), though the sliding amplitude continues to increase during the ramping-up phase up to 400 loading cycles. In the PreTBL series, clear and stable gross sliding conditions are achieved after contact alignment after about a few hundreds or thousands of loading cycles. The misalignment is caused by uneven distribution of the added wear debris, which cannot be avoided with the used method. The solid black line show the reference tests in dry QT-QT conditions [21] with the same sliding amplitude and normal pressure values. In the dry contact conditions, the initial *COF* peaks occur at a value of about 1.4 and decreases over the following ten of thousands of loading cycles until it stabilises at a value of around 0.8.

Fig. 3 shows that the friction peak value decreased in all the experiments. The lowest peak value for COF_{max} occurs with the oils and is about 0.7. With Grease, Paste A and Paste B, the average peak values were about 1.2, 1.1 and 1.3, respectively. The average peak value in the PreCorr series was 1.0. In the PreTBL series, however, there is no friction peak. There was also a delay in the friction peak. The delay ranged from 1000 loading cycles (in the case of Grease) up to 20 000 loading cycles (Paste B). Very low *COF* values occurred before peaking, being about 0.03 at minimum with Pastes A and B. With the exception of the oils, similar levels of steady state COF_{max} values occurred as in the dry contact. Slightly lower values occurred with Paste A, Grease, PreTBL and PreCorr, whereas Paste B had a slightly higher $COF_{\max}$ value. However, the steady state COF_{max} values notably decreased in both oils, being about 0.4, which is a relatively low value and indicates that the lubrication has a clear effect throughout the tests. Fig. 4 presents the COF_{mean} results.

A similar trend is observed in COF_{mean} peak values, as was seen with the COF_{max} values, Fig. 4. The maximum COF_{mean} value in the reference test is about one, and the peak value is lower in every test regardless of the medium. The closest value to the reference test is with Paste B, about 0.7. The peak in oils is again low, about 0.4. Similar behaviour in the delay of the peak also happens. Grease has the shortest delay, whereas the delay increases with the oils, and with Paste B and the PreCorr. The longest delay is in fact with Paste B. However, this paste has the maximum peak value. In the steady state values, all the tests except the PreTBL indicate somewhat decreased values compared to the reference. However, once again, it is the oils that have the lowest values and the COF_{mean} of Oil A is even below 0.2. Fretting loops of different tests during loading are shown in Fig. 5. The sliding amplitude is the result of the angle of the rotation multiplied with contact middle radius.

Non-Coulomb friction can be observed at the beginning of every test except in PreTBL. However, non-Coulomb conditions are mostly declining with increasing load cycles. Especially in the case of Reference, Grease and PreTBL, the shape of the loop at the end of the test resembles ideal-Coulomb loop and the torque is somewhat constant during the gross sliding phase. In the rest of the cases, especially in Paste B, the torque still increases during the gross sliding phase at the end of

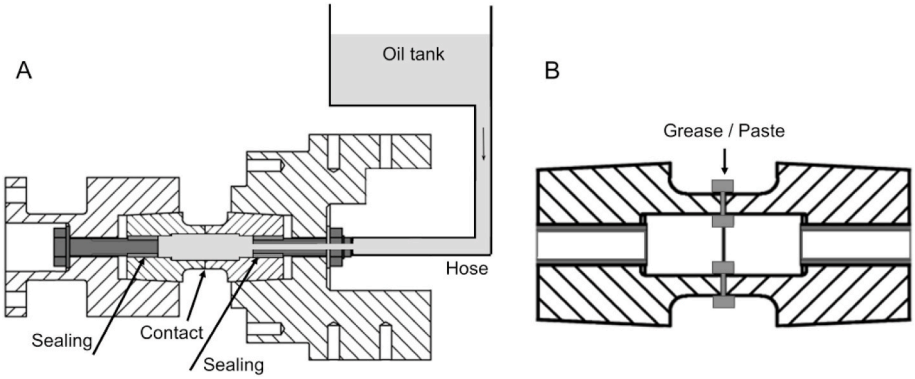

Fig. 2. The arrangements for applying the oils (A) and the pastes and grease (B).

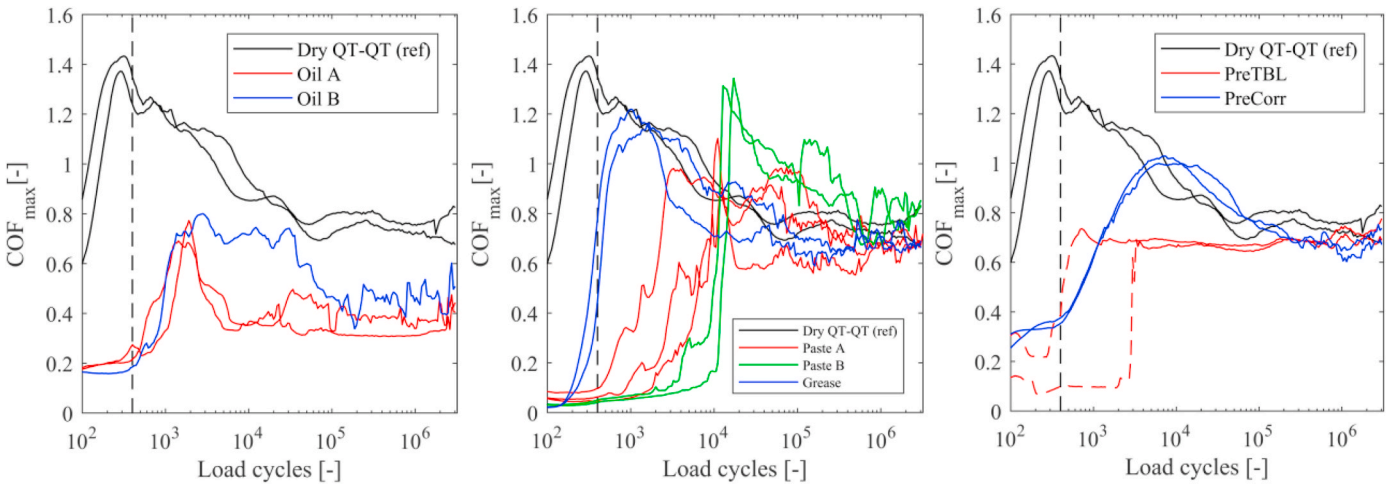

Fig. 3. COF_{max} of all tests and the reference dry QT-QT. The test start-up takes place during the first 400 loading cycles (vertical dotted line).

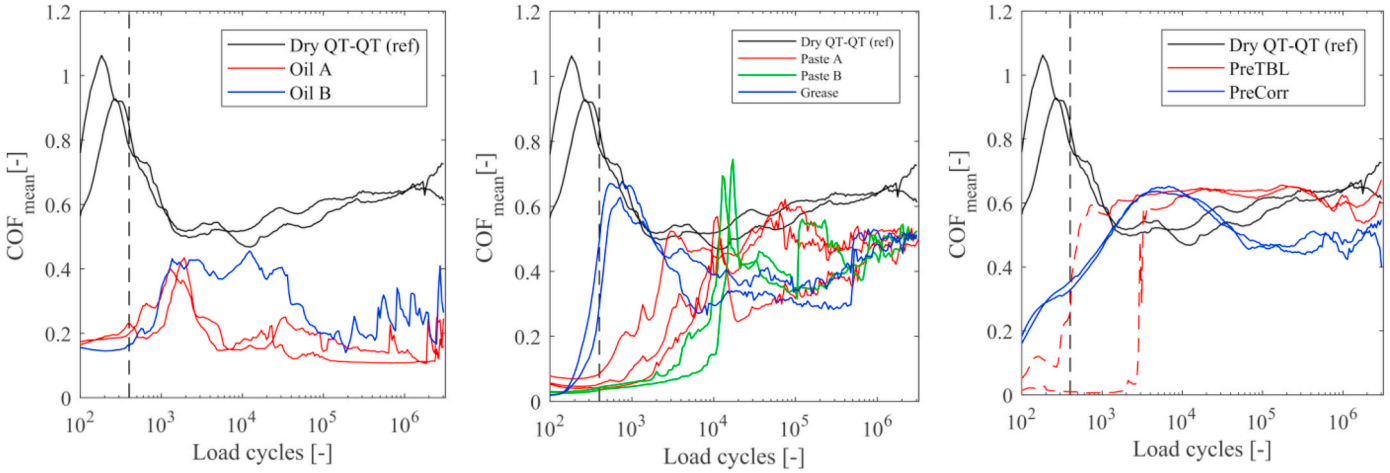

Fig. 4. *COFmean* of all tests and the reference dry QT-QT. The test start-up takes place during the first 400 loading cycles (vertical dotted line). (For interpretation of the references to color in this figure, the reader is referred to the Web version of this article.).

the test. Fig. 6 presents the level of non-Coulombness of the tests (i.e. COF_{max} - COF_{mean}). The average values of ΔCOF of the test series are presented.

In Fig. 6, mostly the peak value decreases compared to the reference. However, with Paste B, a higher peak in ΔCOF occurs and Grease has a similar level of non-Coulombness. ΔCOF values at the stabilized friction regime after some tens of thousands of loading cycles are mostly higher than in the Reference. The exception is the PreTBL, in which the non-Coulombness basically diminishes throughout the tests. With the oils, a large proportion of their friction is due to the non-Coulomb effect. Fig. 7 shows the average frictional energy dissipation of the tests compared to the first reference test. The error bars show the difference between minimum and maximum value of each series.

All the media decreased the frictional energy dissipation compared to the dry reference tests. A clear discrepancy is the values of the oils compared to the other media. Both the oils dissipate only about 20–40% of the energy that the dry contact does. The other cases have closer values to the reference. The values of the individual tests within each series are at reasonably similar levels.

3.2. Fretting scar observations

The fretting scars of the specimens are shown in Fig. 8. A cursory glance of the contact surfaces immediately reveals that fretting damage occurred in every test, demonstrating that none of the pairs of contacting surfaces were completely separated by the media. Compared to the reference tests, there is less reddish-brown coloration, especially with the Grease, Oils and Pastes. The surfaces are greyer and more metallic in colour than they are in the dry contact. This difference in colour indicates changes in the composition of the debris screens. Especially in the Grease, PreTBL, PreCorr and the Paste A and B series, large areas of visually smooth-looking metallic surface exist. There is still quite a lot of intact surface in the Oil A specimen shown in Fig. 8. The fretting scar does not completely cover the contact surface and the grinding marks can be still seen. The most noticeable change in surface topography occurred in the Paste B test, where local protrusions were visible on the surface. These areas might be the reason for the excessive non-Coulombness observed (Fig. 6). However, local damaged regions that seem to be areas of adhesive metal-to-metal scarring can be seen in all of the tests.

EDS data was collected from one specimen of each media, except in PreCorr series from two specimens of a test. Two to four locations were chosen by eye from each individual surface using optical microscope images. 5–10 EDS measurements were taken from each of these locations. This resulted in the total of 144 individual places for oxygen determination. Examples are shown in Fig. 9. As the EDS cannot detect oxygen with high accuracy, rounded values are shown. The locations of these are marked on the surfaces with grey rectangles in Fig. 8.

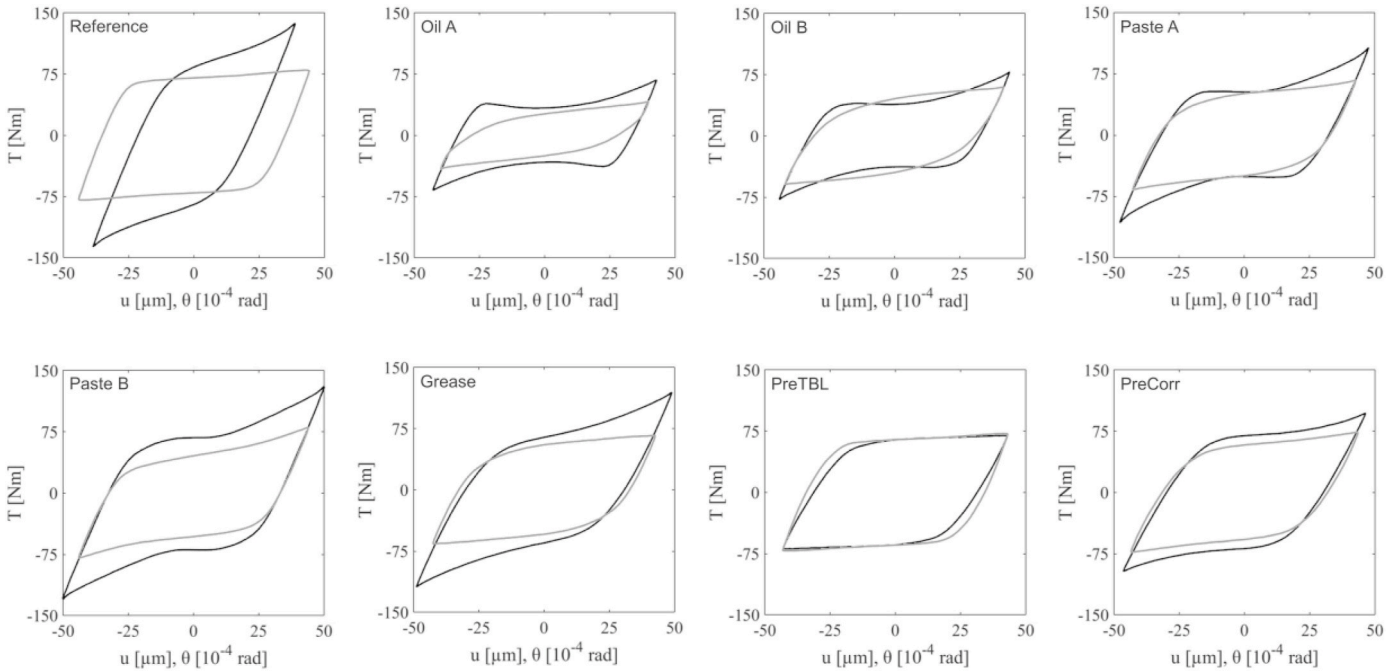

Fig. 5. Fretting loops of different tests at the location of maximum *COFmax* (black line) and at the end of tests (grey line).

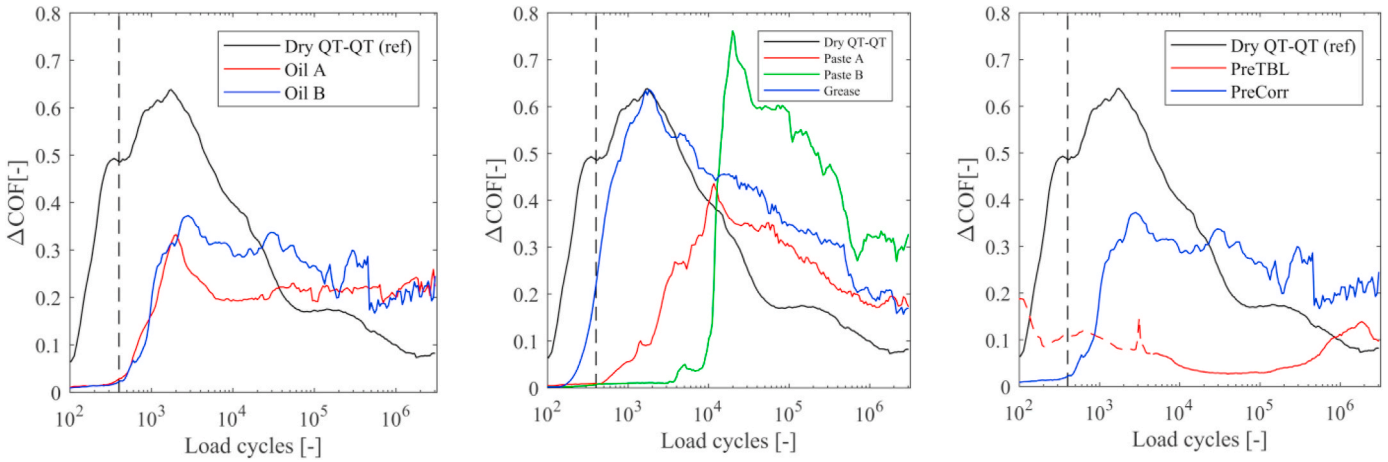

Fig. 6. Δ*COF* of all tests and the reference dry QT-QT. The test start-up takes place during the first 400 loading cycles (vertical dotted line). (For interpretation of the references to color in this figure, the reader is referred to the Web version of this article.).

Secondary electron (SE) images (maximizing topographical contrast) are on the left and backscattered electron (BSE) images (maximizing compositional contrast) on the right with the regions of EDS measurements shown.

The reference scar (Fig. 9A and B) shows typical characteristics observed in dry fretted contact with the self-mated steel pair. Oxide layers with high level of oxidation (over 50 At-%) exist and indication of material transfer can be found. Oxide layers do not cover all the image. Oil B (C-D) shows typical characteristics observed with the lubricants. Different kind of morphology can be seen with signs of plasticity and particulate debris, that typically has no oxygen or only a small amount, as is shown in the figure. In PreTBL (E-F), the whole image is covered with oxidized layer with high amount of oxygen. Cracks can be also seen, perhaps within the oxidized layer without propagation inside the material. PreCorr (G-H) has also widespread oxidized layers with high amount of oxygen. Flaking of the layers can be observed, which may be detached during loading. This behaviour may explain the higher level of wear (Fig. 11) compared to others. Though the amount of carbon cannot be verified with EDS accurately, the two or three times higher amount of carbon in both oils, the grease and both pastes compared to the Reference, PreTBL and PreCorr suggests that the first contacts mentioned have remnants of lubricant. Fig. 10 shows the average amount of oxygen (At-%) in different specimens. The error bars correspond to ±1 standard deviation.

Even though some scatter is present, the results clearly suggest that the oils, pastes and the grease inhibit oxidation, as all of these clearly have a lower amount of average level of oxygen compared to others. In addition, both the pre-corroded and uncorroded specimen have approximately the same amount of oxygen (PreCorr1 and PreCorr2).

3.3. Wear

Wear was quantified in terms of the mass loss of the specimens. The specimens were first weighed before applying any medium, and then again after testing. The individual measurements utilizing a reference weight included five (three in the case of Reference) scalings of each

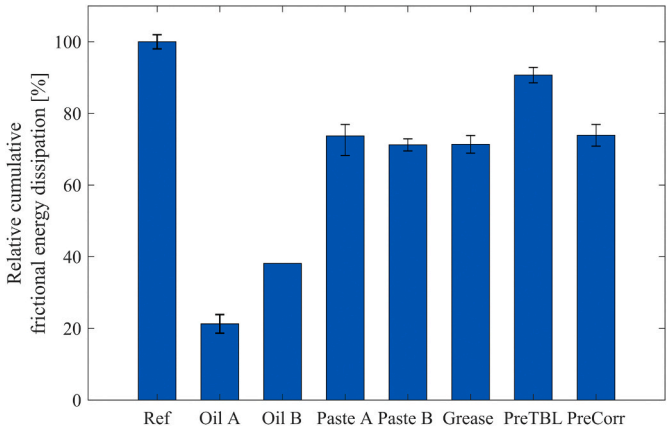

Fig. 7. Relative average frictional energy dissipation of all tests. (For interpretation of the references to color in this figure, the reader is referred to the Web version of this article.).

specimen. The standard deviation of an individual measurement was about 0.5 mg. The average values were used and the mass losses of both specimens were calculated and the average mass losses are shown in Fig. 11. In the PreCorr series, the mass losses of the un-corroded counter specimens are reported. The error bars show the difference between minimum and maximum mass values.

Compared to the reference specimens, on average the oils and also the PreTBL decreased wear. However, Pastes A and B and the Grease had slightly more wear than the dry contact. The most worn was one of the PreCorr specimens. Paste B wore more than Paste A. Similar results were obtained in Ref. [32], where an MoS2-lubricated contact wore more than one which had graphite lubrication. There were quite large differences in the mass losses of the specimens. The negative mass loss values of some individual specimens, especially in one of Paste B tests, indicate the occurrence of material transfer between the specimens.

Fig. 12 show the mass losses as a function of average frictional energy dissipation during a loading cycle (A) and the level of non-Coulombness (B). As Fig. 12 shows, the wear here cannot be explained by the increased frictional energy dissipation. Similar results was achieved in Ref. [11], where the plain approach of frictional energy dissipation did not correlate with the wear that occurred with lubricated specimens, though the developed effective frictional energy dissipation did. However, the level of non-Coulombness has quite a good correspondence with the amount of wear. The higher the level of non-Coulombness, the higher the mass loss. It might be that tangential interlocking and material transfer play a major role in wear behaviour. The low wear in the PreTBL series could be explained by the velocity accommodation of the third-body-layer.

4. Discussion

All the studied media and intermediate layers decreased the maximum value of the initial friction peak in gross sliding conditions compared to the dry self-mated QT-QT contact. In the dry contact, the peak is already reached after only a few hundred loading cycles. A delay occurred in all cases, ranging from about 1000 loading cycles to about 20 000 loading cycles. In these delayed cases, there was typically a very low *COF* before the peak, indicating efficient lubrication. With the exception of the molybdenum sulphide paste, the non-Coulombness was lower during the initial friction peak, and the same was true for the graphite grease. The lower values indicate a decreased amount of adhesive wear during the initial loading cycles and the associated formation of tangentially interlocked features. Indeed, the biggest interlocked feature was found with the molybdenum sulphide paste. Basically, in most cases the steady state *COF* (both COF_{max} and COF_{mean}) did not change much in comparison to the dry reference contact, although there were slight differences. At steady state *COF,* the artificial debris layer had virtually no non-Coulombness at all, while the dry contact had the second lowest level of non-Coulombness.

The oils, grease and pastes all have lubricating properties that can

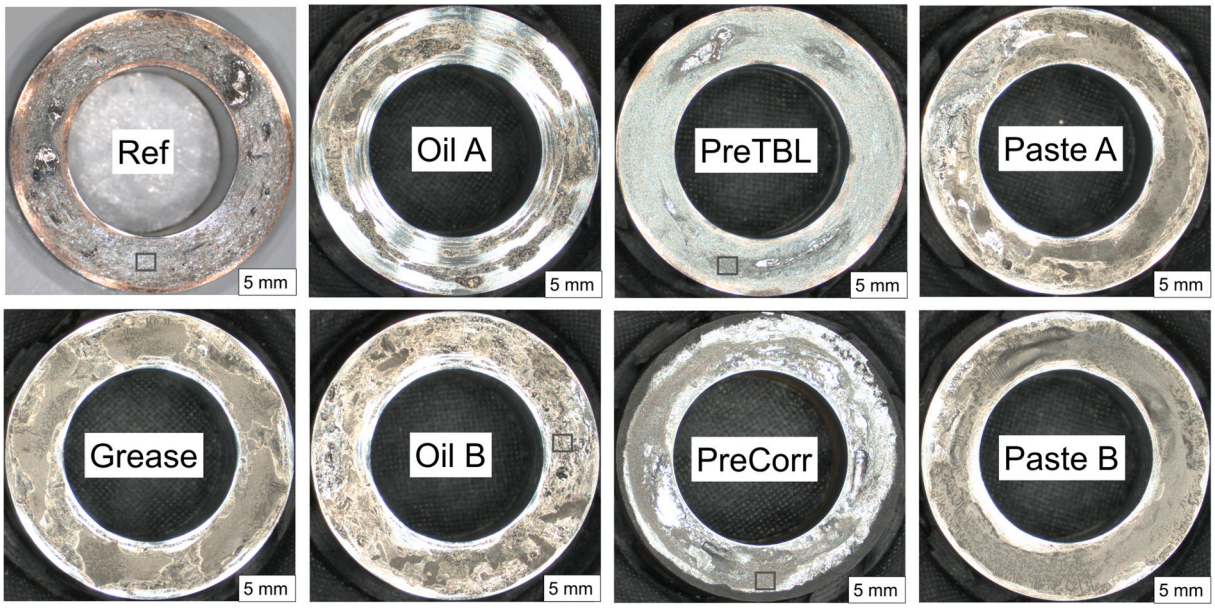

Fig. 8. Fretting scars. (For interpretation of the references to color in this figure, the reader is referred to the Web version of this article.).

explain the decreased *COF*. The oils decreased both the initial and the steady state *COF*s notably. The low *COF,* especially at the beginning, indicates very good lubrication conditions in the oils. Some delayed friction peaks exist but they are not that high. The magnitudes of the *COF*s (0.2–0.3) indicate boundary lubrication in some dry adhesive contacts. Oil additives may also play a role. The low *COF* levels are sustained and indicate oil penetration, so it seems that oil may be available all the time in the contact interface. The oils seem to be able to provide lubricant media in the long term, which results in lower *COF*s with milder surface damage. The *COF* and the level of fretting scar coverage were higher with Oil B than with Oil A, and this suggests that the lower-viscosity oil lubricates the contact better. This could be explained by the better penetration of the lower-viscosity oil. Generally speaking, lower *COF* results in decreased stresses. However, in practice a low *COF* may lead to higher slip, and this may also restrict the amount of forces that could be transmitted.

The grease, and especially the pastes, only seem to provide good lubrication during the initial loading cycles, after which the *COF* increases and peaks. The grease had graphite and EP additives, but the actual temperature in the contact interface is not known and it is possible that the required temperature is not reached and thus the additives are not activated. Regarding the differences in the viscosities of the two oils, one would not expect the results obtained [12], to show much difference in *COF* and wear. Nevertheless, the higher *COF*s of the

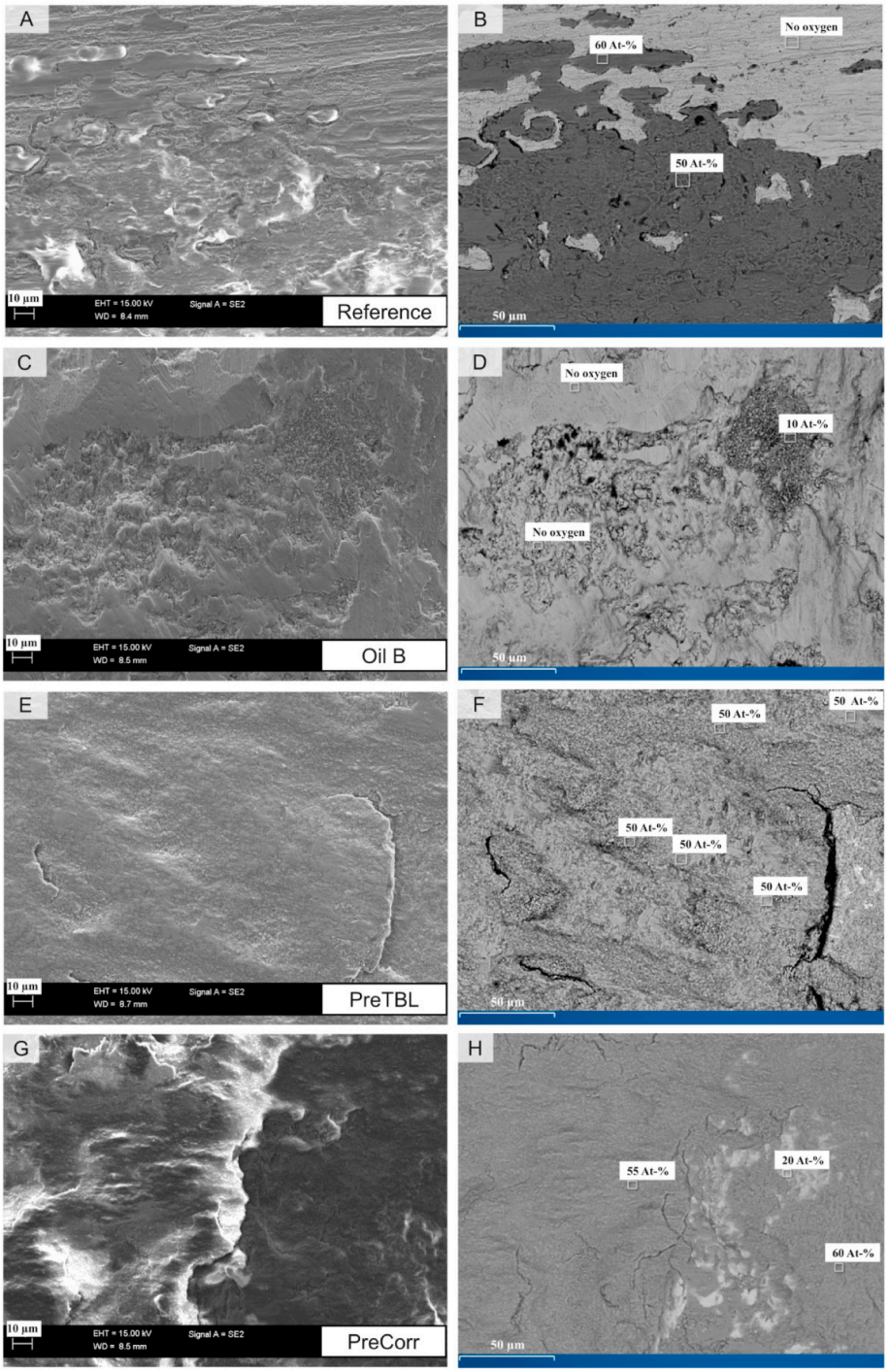

Fig. 9. Fretting scar SEM-micrographs (SE and BSE, from the same location) with EDS.

Pastes and the Grease suggest a possible relation between viscosity and *COF*. It seems that the pastes and grease are mostly squeezed out from the contact and are not able to make their way back. This indicates that the initial lubrication layer sooner or later disappears in a local contact, which tends to have metal-metal contacts. In principle, a wide variation in the *COF* is not good for contacts in practice, as the *COF* may initially be too low leading to excessive slippage, and then as it increases it can lead to surface damage. High levels of non-Coulombness and wear were measured with these, including local adhesion spots.

In the series where the artificial debris layer was added before testing, the friction peak completely disappeared and there was no non-Coulombness. This indicates that the debris layer prevented the first bodies to contact and remarkably decreased both the initial adhesion and also the wear. Although surface damage can still be observed, there is no excessive creation of adhesion spots. Furthermore, the *COF* behaviour is relatively stable and the steady-state *COF* is the same as for the reference case, so the contact seems to reach steady state friction and wear mode almost instantly, without any adhesion at the beginning. The reasonable level and stable *COF*s achieved are good for practical fretting contact design. The artificial debris layer basically acts as a solid lubricant (velocity accommodation), thus decreasing *COF*. The same phenomenon might be happening with the pre-corroded tests, as the corrosion products act as solid lubricant on the otherwise dry contact surface. It may be assumed that in both cases, but especially in the first

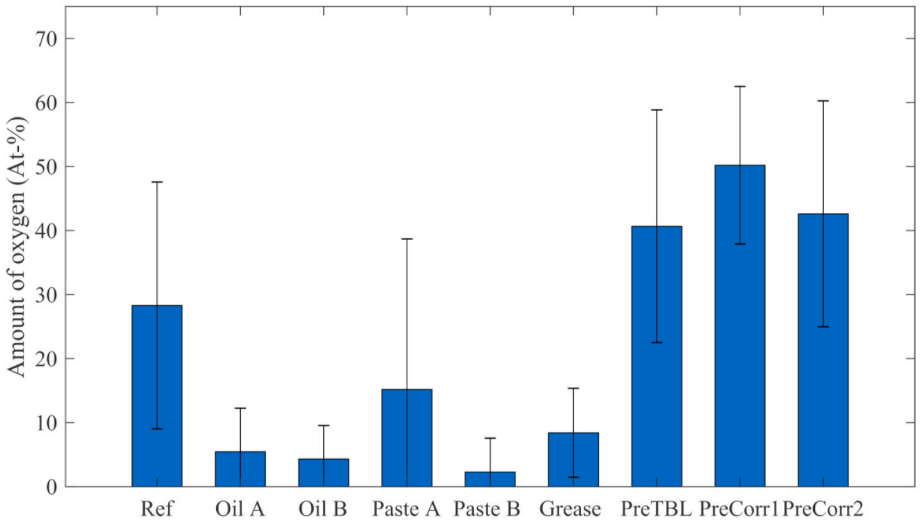

Fig. 10. Amount of oxygen (At-%).

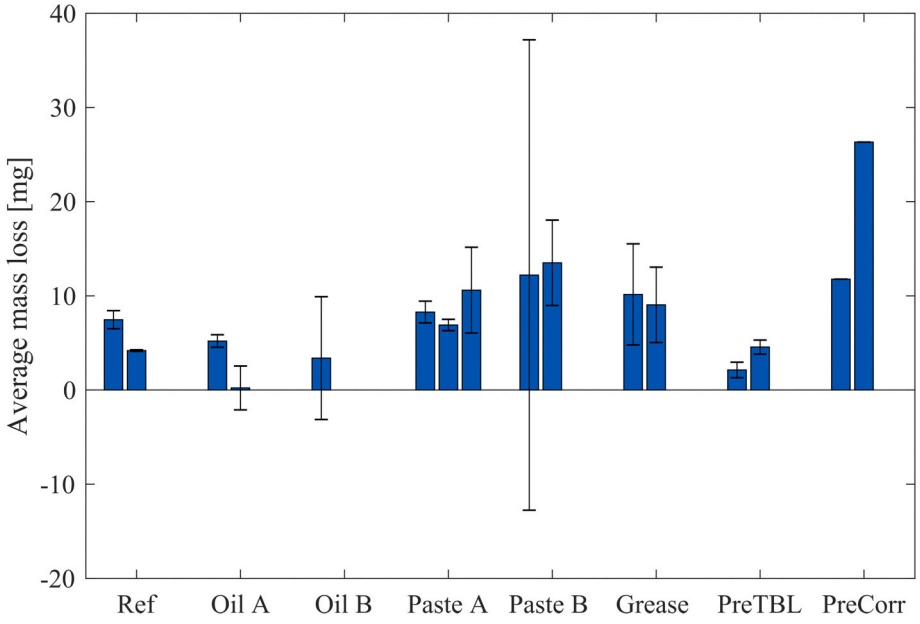

Fig. 11. Average mass losses of the experiments. (For interpretation of the references to color in this figure, the reader is referred to the Web version of this article.).

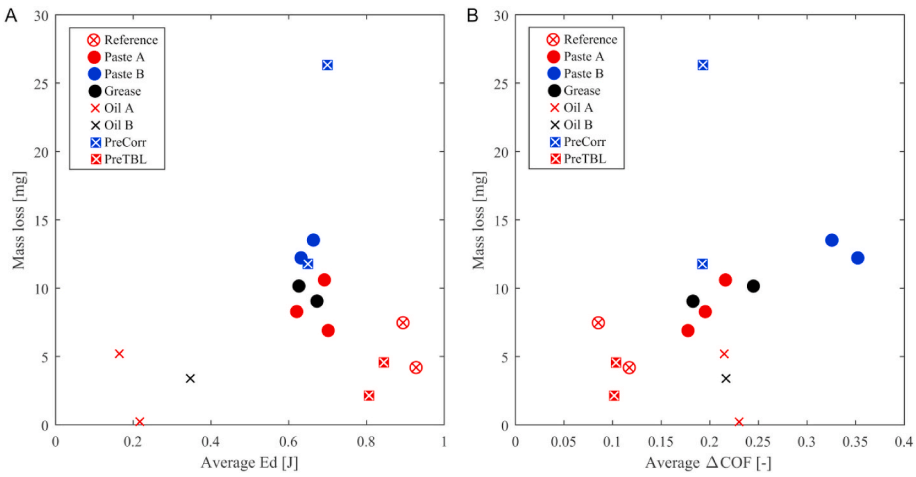

Fig. 12. Mass losses of the specimens as a function of average frictional energy dissipation (A) and average difference between COF_{max} and COF_{mean} (B). (For interpretation of the references to color in this figure, the reader is referred to the Web version of this article.).

case, the fretting motion is mostly accommodated by the formation of the third body, thus lowering the *COF*. Indeed, in the pre-corroded test series, the friction peak also greatly decreased, but local spots of adhesive wear damage occurred on the surface. However, the steady state *COF* remained unchanged in this case, too.

The level of average non-Coulombness corresponded reasonably well with wear in terms of mass losses, but the plain accumulated frictional energy dissipation did not. The oil test specimens had somewhat fewer areas of fretting scar than the other specimens, and also had the lowest *COF* and the lowest level of average frictional energy dissipation. The tests with the oils, pastes and the grease seemed to result in less oxidation as measured by SEM-EDS and also indicated by the amount of reddish-brown discoloration, and this obviously is due to the oxygen 'sealing effect'. As the space inside the specimens is filled with oil, this should limit the amount of oxygen that can enter the inside of the contact. On the other hand, the specimen's outer surfaces are exposed to air, so different levels of oxidation might be expected at the inner and outer edges, but this kind of behaviour was not observed. As motion occurs between the two flat-ended surfaces without any movement applied in the normal direction, it is clear that full film lubrication cannot exist in principle. Furthermore, the lack of clearance between the precisely manufactured contacting surfaces, or the very small clearances within the small surface roughness scale might be enough of a barrier to prevent the lubricant from entering the contact.

5. Conclusions

Dry fretting contact with steels is characterized by a high initial friction peak in gross sliding conditions. This leads to adhesive surface damage and non-Coulomb friction. Different media were studied in similar fretting conditions to prevent friction from peaking. These media were two different oils, one grease, two pastes, an artificial wear debris layer and a pre-corroded layer. The main conclusions of the study are as follows:

- All the media, expect the grease, notably decreased the initial friction peak compared to the dry reference case.
- The artificial wear debris layer eliminated the friction peak completely. It also had large areas of smooth fretted surface that could be seen by visual inspection.
- The frictional behaviours were characterized by a delay in the peak ranging from some hundreds of loading cycles up to twenty thousand loading cycles. Low coefficient of friction (*COF*) values were measured before the peak in some cases, indicating good initial lubrication.
- Exceptionally, the oils had relatively low *COF* throughout the tests. The steady state *COF*s with the other media were on much the same level as with the reference (0.7–0.8). The oils clearly dissipated less frictional energy than the other media.
- One paste had higher level of non-Coulombness than the reference, but the others had lower values.
- Fretting scars and damage were observed in every test. It is possible that the lubricants may seal the contact interface, thus decreasing the level of oxidation, as indicated by EDS measurements.
- There was reasonable agreement between the amount of wear and the level of non-Coulombness.

Declaration of competing interest

The authors declare that they have no known competing financial interests or personal relationships that could have appeared to influence the work reported in this paper.

Acknowledgements

The authors are grateful for the financial support provided by Business Finland Oy (formerly Tekes) in the form of research projects ISA (Dnro 7204/31/2018), MaNuMiES (Dnro 3361/31/2015) and WIMMA (Dnro 1566/31/2015) and Wärtsilä Finland Oy. The FESEM-EDS work made use of Tampere Microscopy Center facilities at Tampere University. Mari Honkanen carried out the work and Leevi Kurki helped with sample preparation.

References

[1] J. Hintikka, J. Juoksukangas, A. Lehtovaara, T. Frondelius, A. Mäntylä, Non-idealities in fretting contacts, J. Struct. Mech. 50 (3) (2017) 171–174, https://doi.org/10.23998/rm.64886.
[2] Z.R. Zhou, L. Vincent, Lubrication in fretting - a review, Wear 225–229 (1999) 962–967, https://doi.org/10.1016/S0043-1648(99)00038-1.
[3] Z.A. Wang, Z.R. Zhou, G.X. Chen, An investigation of palliation of fretting wear in gross slip regime with grease lubrication, Ind. Lubric. Tribol. 63 (2) (2011) 84–89, https://doi.org/10.1108/00368791111112207.
[4] M. Eriten, A.A. Polycarpou, L.A. Bergman, Effects of surface roughness and lubrication on the early stages of fretting of mechanical lap joints, Wear 271 (11–12) (2011) 2928–2939, https://doi.org/10.1016/j.wear.2011.06.011.
[5] I.R. McColl, R.B. Waterhouse, S.J. Harris, M. Tsujikawa, Lubricated fretting wear of a high-strength eutectoid steel rope wire, Wear 185 (1–2) (1995) 203–212, https://doi.org/10.1016/0043-1648(95)06616-0.
[6] T. Maruyama, T. Saitoh, A. Yokouchi, Differences in mechanisms for fretting wear reduction between oil and grease lubrication, Tribol. Trans. 60 (3) (2017) 497–505, https://doi.org/10.1080/10402004.2016.1180469.
[7] S.M. Wang, H. Gao, M. Xu, Investigation of grease lubrication effects on the fretting wear behavior of ball bearings, Adv. Mater. Res. 291–294 (2011) 1491–1495. https://doi.org/10.4028/www.scientific.net/AMR.291-294.1491.

[8] Z.R. Zhou, Q.Y. Liu, M.H. Zhu, L. Tanjala, Ph. Kapsa, L. Vincent, Investigation of fretting behaviour of several metallic materials under grease lubrication, Tribol. Int. 33 (2) (2000) 69–74, https://doi.org/10.1016/S0301-679X(99)00100-0.
[9] R.B. Waterhouse, Fretting Corrosion, 1st, Pergamon press, Oxford, 1972.
[10] Q.Y. Liu, Z.R. Zhou, Effect of displacement amplitude in oil-lubricated fretting, Wear 239 (2) (2000) 237–243, https://doi.org/10.1016/S0043-1648(00)00323-9.
[11] L. Haviez, S. Fouvry, R. Toscano, G. Yantio, An energy-based approach to understand the effect of fretting displacement amplitude on grease-lubricated interface, Wear 338–339 (2015) 422–429, https://doi.org/10.1016/j.wear.2015.07.015.
[12] M. Shima, H. Suetake, I.R. McColl, R.B. Waterhouse, M. Takeuchi, On the behaviour of an oil lubricated fretting contact, Wear 210 (1–2) (1997) 304–310, https://doi.org/10.1016/S0043-1648(97)00078-1.
[13] W. Qin, M. Wang, W. Sun, P. Shipway, X. Li, Modeling the effectiveness of oil lubrication in reducing both friction and wear in a fretting contact, Wear 426–427 (2019) 770–777, https://doi.org/10.1016/j.wear.2019.02.029.
[14] J. Xu, Z.R. Zhou, C.H. Zhang, M.H. Zhu, J.B. Luo, An investigation of fretting wear behaviors of bonded solid lubricant coatings, J. Mater. Process. Technol. 182 (1–3) (2007) 146–151, https://doi.org/10.1016/j.jmatprotec.2006.07.023.
[15] M. Godet, Third-bodies in tribology, Wear 136 (1) (1990) 29–45, https://doi.org/10.1016/0043-1648(90)90070-Q.
[16] Y. Berthier, L. Vincent, M. Godet, Velocity accommodation in fretting, Wear 125 (1–2) (1988) 25–38, https://doi.org/10.1016/0043-1648(88)90191-3.
[17] M. Varenberg, G. Halperin, I. Etsion, Different aspects of the role of wear debris in fretting wear, Wear 252 (11–12) (2002) 902–910, https://doi.org/10.1016/S0043-1648(02)00044-3.
[18] P. Zhang, X. Liu, W. Lu, W. Zhai, M. Zhou, J. Wang, Fretting wear behavior of CuNiAl against 42CrMo4 under different lubrication conditions, Tribol. Int. 117 (2018) 59–67, https://doi.org/10.1016/j.triboint.2017.08.013.
[19] H. Ding, G. Zhou, Z. Dai, Y. Bu, T. Jiang, Corrosion wear behaviors of 2024Al in artificial rainwater and seawater at fretting contact, Wear 267 (1–4) (2009) 292–298, https://doi.org/10.1016/j.wear.2008.11.031.
[20] V. Périer, L. Dieng, L. Gaillet, C. Tessier, S. Fouvry, Fretting-fatigue behaviour of bridge engineering cables in a solution of sodium chloride, Wear 267 (1–4) (2009) 308–314, https://doi.org/10.1016/j.wear.2008.12.107.
[21] J. Hintikka, A. Lehtovaara, A. Mäntylä, Fretting-induced friction and wear in large flat-on-flat contact with quenched and tempered steel, Tribol. Int. 92 (2015) 191–202, https://doi.org/10.1016/j.triboint.2015.06.008.
[22] J. Juoksukangas, V. Nurmi, A. Lehtovaara, M. Honkanen, M. Vippola, J. Hintikka, A. Mäntylä, J. Vaara, T. Frondelius, Formation and characterization of cracks and degradation layers in large flat-on-flat fr>etting contact, in: 9th Int. Symp. Frett. Fatigue, 1.-3.4.2019, Seville, Spain, University of Seville, 2019, pp. 1–2.
[23] J. Juoksukangas, V. Nurmi, J. Hintikka, M. Honkanen, M. Vippola, A. Lehtovaara, A. Mäntylä, J. Vaara, T. Frondelius, Cracks and degradation layers in large flat-on-flat fretting contact with steels and cast iron, Tribol. Int. 145 (2020), https://doi.org/10.1016/j.triboint.2019.106102.
[24] J. Hintikka, A. Lehtovaara, A. Mäntylä, Normal displacements in non-Coulomb friction conditions during fretting, Tribol. Int. 94 (2016) 633–639, https://doi.org/10.1016/j.triboint.2015.10.029.
[25] J. Juoksukangas, A. Lehtovaara, A. Mäntylä, Experimental and numerical investigation of fretting fatigue behavior in bolted joints, Tribol. Int. 103 (2016) 440–448, https://doi.org/10.1016/j.triboint.2016.07.021.
[26] V. Nurmi, J. Hintikka, J. Juoksukangas, M. Honkanen, M. Vippola, A. Lehtovaara, A. Mäntylä, J. Vaara, T. Frondelius, The formation and characterization of fretting-induced degradation layers using quenched and tempered steel, Tribol. Int. 131 (2019) 258–267, https://doi.org/10.1016/j.triboint.2018.09.012.
[27] J. Juoksukangas, V. Nurmi, J. Hintikka, M. Vippola, A. Lehtovaara, A. Mäntylä, J. Vaara, T. Frondelius, Characterization of cracks formed in large flat-on-flat fretting contact, Int. J. Fatig. 124 (2019) 361–370, https://doi.org/10.1016/j.ijfatigue.2019.03.004.
[28] J. Hintikka, A. Mäntylä, J. Vaara, T. Frondelius, A. Lehtovaara, Running-in in fretting, transition from near stable friction regime to gross sliding, in: 9th Int. Symp. Frett. Fatigue, 1.-3.4.2019, Seville, Spain, University of Seville, 2019, pp. 1–2.
[29] J. Hintikka, A. Mäntylä, J. Vaara, T. Frondelius, J. Juoksukangas, A. Lehtovaara, Running-in in fretting, transition from near-stable friction regime to gross sliding, Tribol. Int. 143 (2020) 1–9, https://doi.org/10.1016/j.triboint.2019.106073.
[30] J. Hintikka, A. Mäntylä, J. Vaara, T. Frondelius, A. Lehtovaara, Stable and unstable friction in fretting contacts, Tribol. Int. 131 (2019) 73–82, https://doi.org/10.1016/j.triboint.2018.10.014.
[31] J. Juoksukangas, J. Hintikka, A. Lehtovaara, A. Mäntylä, J. Vaara, T. Frondelius, Avoiding the high friction peak in fretting contact, J. Struct. Mech. 53 (1) (2020) 1–8, https://doi.org/10.23998/rm.76266.
[32] A. Neyman, J. Sikora, Grease effect on fretting wear of mild steel, Ind. Lubric. Tribol. 60 (2) (2008) 67–78, https://doi.org/10.1108/00368790810858368.